CHEMISTRY OF MATERIALS

pubs.acs.org/cm Article

Synthesis and Structural Study of Substituted Ternary Nitrides for Ammonia Production

Xiang Gao, H. Evan Bush, James E Miller, Alicia Bayon, Ivan Ermanoski, Andrea Ambrosini, and Ellen B. Stechel*

Cite This: https://doi.org/10.1021/acs.chemmater.3c00606 Read Online

ACCESS | Metrics & More | Article Recommendations | Supporting Information

ABSTRACT: Over the past few decades, inorganic nitride materials have grown in importance in part due to their potential as catalysts for the synthesis of NH_3, a key ingredient in fertilizer and precursor to industrial chemicals. Of particular interest are the ternary (ABN) or higher-order nitrides with high metal-to-nitrogen ratios that show promise in enhancing NH_3 synthesis reaction rates and yields via heterogeneous catalysis or chemical looping. Although metal nitrides are predicted to be numerous, the stability of nitrogen triple bonds found in N_2, especially in comparison to the metal−nitrogen bonds, has considerably hindered synthetic efforts to produce complex nitride compounds. In this study, we present an exhaustive down-selection process to identify ternary nitrides for a promising chemical looping NH_3 production mechanism. We also report on a facile and efficient two-step synthesis method that can produce well-characterized η-carbide Co_3Mo_3N/Fe_3Mo_3N or filled β-manganese Ni_2Mo_3N ternaries, as well as their associated quaternary, $(Co,Fe)_3Mo_3N$, $(Fe,Ni)_2Mo_3N$, and $(Co,Ni)_2Mo_3N$, solid solutions. To further explore the quaternary space, syntheses of $(Co,Ni)_3Mo_3N$ (Ni ≤ 10 mol %) and $Co_3(Mo,W)_3N$ (W ≤ 10 mol %) were also investigated. The structures of the nitrides were characterized via X-ray powder diffraction. The morphology and compositions were characterized with scanning electron microscopy. The multitude of chemically unique, but structurally related, nitrides suggests that properties such as nitrogen activity may be tunable, making the materials of great interest for NH_3 synthesis schemes.

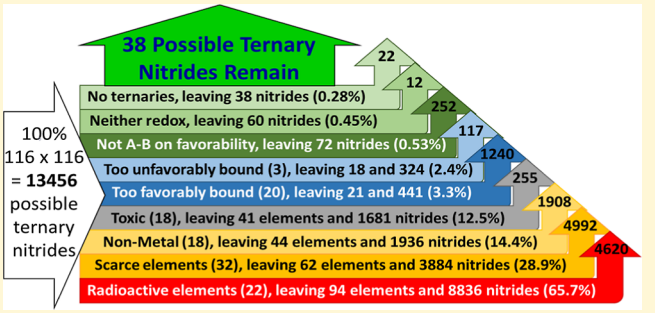

INTRODUCTION

Nitrogen is one of the essential elements in all living organisms, found in proteins, DNA, and chlorophyll. Though nitrogen is abundant in the atmosphere as molecular N_2, the strength of the N_2 triple bond and its stable electron configuration render molecular nitrogen inaccessible for most organisms. The most challenging and rate-limiting step in the ecological nitrogen cycle is fixation—converting N_2 gas into simple and reactive nitrogen compounds such as NH_3 and NO, precursors for complex synthesis or biosynthesis of biologically essential nitrogen compounds.

Nitrogen fixation was also a major challenge to agricultural productivity until the Haber−Bosch (H−B) process, which produces NH_3 from H_2 and N_2, became industrial viable in 1913.[1] The high-pressure (150−200 atm) conversion of molecular N_2 and H_2 into NH_3 via H−B enabled the mass production of nitrogen fertilizers, sustaining a growing human population to this day. Currently, about 2% of the world's natural gas output is utilized to produce the H_2 feed gas via steam methane reforming and the N_2 feed gas by removing O_2 from air (converting it to CO_2 and H_2O). The H−B ammonia synthesis reaction is exothermic and thermodynamically favorable at low temperatures. However, the reaction kinetics are slow at these temperatures. Therefore, current industrial NH_3 production occurs at higher temperatures, where the chemical equilibrium significantly favors H_2 and N_2 over NH_3. This unfavorable equilibrium is compensated for by operating at high pressures and by the recycling of gasses, both of which consume energy, often of fossil origin. Global demand for fixed nitrogen continued to rise, and by early 2022, nitrogen fertilizer prices reached an all-time high due to tight supplies world-wide and rising prices for natural gas, the principal raw material. Currently, extensive use of the H−B process consumes more than 1% of the world's total energy production and emits more than 300 million tons of CO_2 annually.[2] The carbon-intensive nature and continually increasing demand for NH_3 warrant a search for a new, more sustainable process.

There have been many studies on alternatives to H−B for nitrogen fixation, but, to date, these technologies have been

Received: March 17, 2023
Revised: July 5, 2023

Downloaded via SANDIA NATL LABORATORIES on July 21, 2023 at 17:52:27 (UTC).
See https://pubs.acs.org/sharingguidelines for options on how to legitimately share published articles.

ACS Publications © XXXX American Chemical Society

considered non-competitive. Of note, renewably powered non-thermal plasma technology[3] is an environmentally benign alternative but faces challenges in plasma catalysts, energy conversion, and reactor engineering. The enhancement of biological nitrogen fixation[4,5] by improving nitrogenase enzymes is also environmentally benign. Other promising routes include metallocomplexed nitrogen fixation[6,7] catalytic cycles or photochemical nitrogen reduction to convert dinitrogen molecules into dinitrogen complexes or NH_3. These approaches are not yet amenable to up-scaling and commercialization due to low yields, extremely expensive and relatively short-lived catalysts, and high energy consumption.

Over the last decade, NH_3 synthesis based on thermochemical cycles has also gained interest. Michalsky and Pfromm[8] proposed a solar thermochemical process operated at ambient pressure via a "nitridation−hydrolysis−chemical reduction by H_2" cycle with chromium oxide/nitride that produced trace amounts of NH_3 during Cr_2N hydrolysis. The group also evaluated the thermodynamic and economic feasibility of using a MoO_2/Mo_2N pair in a two-step solar thermochemical synthesis of NH_3, conducted at or below 1500 K.[9] Recently, they proposed the concept of chemical looping[10,11] between a metal nitride and its metallic counterpart by alternating between H_2 and N_2 sources and demonstrated NH_3 production via Mn-based binary nitrides. The studies established critical fundamentals for constructing novel cycles aimed at utilizing the solid-state lattice nitrogen in metal nitrides to form NH_3. However, the thermodynamic and experimental evaluations were limited to binary (MN) nitrides, and the capability for nitride regeneration within such cycles was not fully elucidated. In this context, ternary (ABN) nitrides are promising, especially if their lattice nitrogen activity (i.e., thermodynamics and kinetics) can be tuned to be more favorable compared to binaries.

Ternary nitrides, including Co_3Mo_3N, Fe_3Mo_3N, or Ni_2Mo_3N, have been demonstrated to be efficient H−B catalysts. The most active catalyst, Co_3Mo_3N impregnated with 2 mol % Cs as a promoter, has been shown to be twice as active as commercial iron-based catalysts and is more resistant to deactivation.[12−14] Apart from heterogeneous catalysis, under appropriate conditions, these η-carbide structured ternary nitrides can also act as nitrogen reservoirs and be used to produce NH_3 via hydrogenation of the bulk lattice nitrogen. One such material, Co_3Mo_3N, which crystallizes in the η-6 carbide structure, reduces (loses N) in the presence of H_2 at elevated temperatures to yield NH_3. The material converts to Co_6Mo_6N with the η-12 carbide structure in the process through a reordering of half the nitrogen atoms from the 16c to the 8a Wyckoff site. In turn, Co_3Mo_3N can be regenerated from Co_6Mo_6N by switching the gas from H_2 to a H_2/N_2 mixture, or even N_2 alone.[15] These two reactions (eqs 1 and 2) form the basis of a novel chemical looping approach to NH_3 synthesis:

$$2Co_3Mo_3N + 1.5H_2 \rightarrow Co_6Mo_6N + NH_3 \quad (1)$$

$$Co_6Mo_6N + 0.5N_2 \rightarrow 2Co_3Mo_3N \quad (2)$$

The net reaction of eqs 1 and 2 is the ammonia synthesis (H−B) reaction, which is mildly exothermic. This chemical looping approach should be amenable to integration with green resources, including green H_2 and N_2, and renewable energy input. A solar thermochemical process that encompasses H_2 and N_2[16−18] production while supplying energy for the above chemical looping approach, for example, may be a promising candidate for carbon-neutral NH_3 synthesis.

One challenge to efficient NH_3 production via chemical looping is developing a family of nitrides with tunable nitrogen activity (thermodynamics) to enable process optimization. Suitable candidates should support direct NH_3 synthesis in the presence of H_2 (eq 1) and the subsequent re-nitridation in the presence of N_2 (eq 2). For process simplification and efficiency, both reactions would ideally proceed without large temperature swings and at total pressures much lower than in H−B. However, in the context of a two-step cyclic reaction, engineering one step will inevitably constrain the other because the thermodynamics of the individual reactions must sum to that of the H−B reaction. Thus, it is generally true for a given material that the more thermodynamically favorable the nitride formation overall, the less favorable the ammonia formation, and vice versa. Figure 1 shows the reaction couples for two

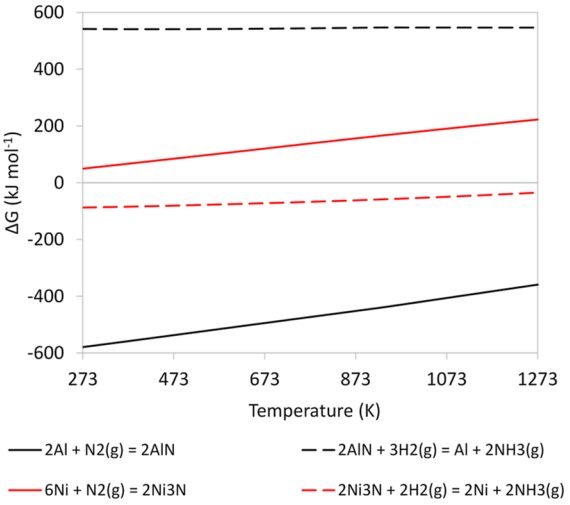

Figure 1. Gibbs free energy as a function of temperature for nitridation and ammonia synthesis for Al/AlN and Ni/Ni_3N pairs illustrating the inverse thermodynamic coupling of the two. Comparing the two couples, it is clear that the more favorable (more negative ΔG) one of the reactions, the less favorable is its complement. In a given case, either of the two reactions, nitridation and ammonia formation, may be the more thermodynamically favorable. For Al, nitride formation is the most favorable, while for Ni, ammonia formation is the most favorable.

binary nitrides at relevant temperatures illustrating this principle. Nitride formation is far more favorable for Al than for Ni, however ammonia formation is far more favorable for Ni than for Al. The extent of the difference in this example is such that the reaction couples are flipped relative to one another, i.e., ΔG is negative (thermodynamically favorable) for nitride formation in one case, and ammonia formation in the other. Note that, while reaction parameters such as temperature and pressure may be manipulated, the binary materials themselves offer nothing in way of thermodynamic tunability. This suggests the need to explore a more complex materials space, e.g., ternary nitrides (ABN), guided by the concept of combining the thermodynamics of separate binaries to achieve intermediate thermodynamic properties.

Regarding terminology, the ABN convention for ternary nitrides is widely adopted in the literature[19−22] and does not limit A-group and B-group definitions to the context of cation location in the crystal structure. Here, we adopt the same ABN

https://doi.org/10.1021/acs.chemmater.3c00606
Chem. Mater. XXXX, XXX, XXX−XXX

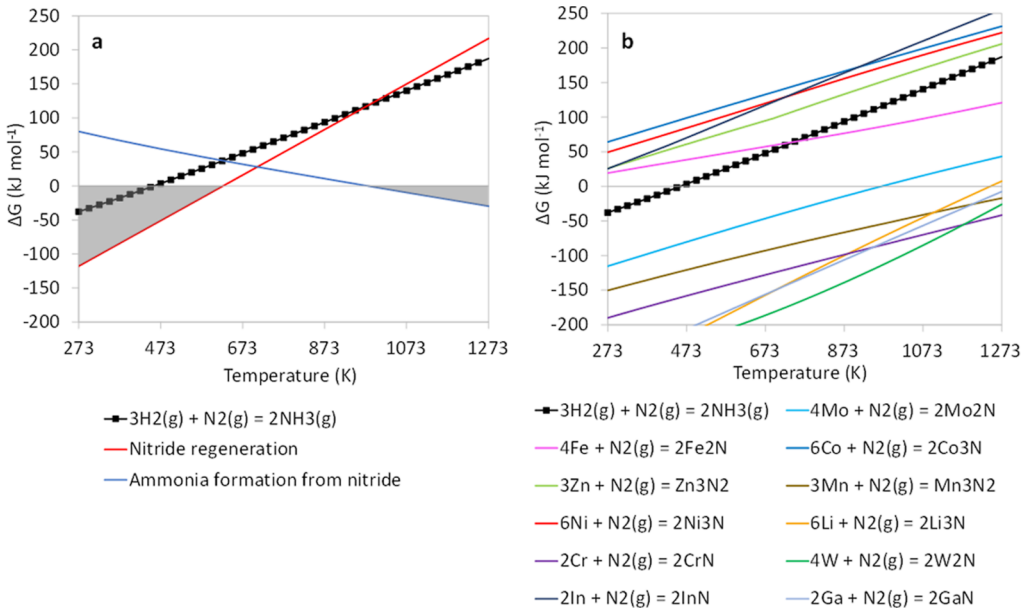

Figure 2. Gibbs free energy changes for (a) the ideal case of a two-step thermochemical cycle (blue and red) to replace the ammonia synthesis reaction (black with squares). (b) Nitride formation via reaction of metals with N_2 compared to the conventional ammonia synthesis reaction. Data from HSC Chemistry 9, Outotec, Finland.

convention for ternaries, but refer to A and B groups according to their difference in thermodynamics, on which we elaborate in the following sections.

A number of studies on ternary nitride synthesis have been reported. Laassiri et al., studied the synthesis of manganese nitride-based materials (AMnN, A = Fe, Co, K, Li) using $NaNH_2$ as the reactive nitrogen source.[23] Mo-based materials have also been synthesized and reported as catalysts for H−B synthesis, including Co_3Mo_3N, Fe_3Mo_3N, and Ni_2Mo_3N, and their reaction mechanisms have been modeled. However, few systematic experimental investigations[24−26] of A-group and B-group substitutions and their effect on the ternary nitride structural compositions have been reported.

In this work, we present thermodynamic and practical motivations that drive the selection of ternary nitride candidates for the proposed chemical looping process. We also describe the synthesis of a series of ternary nitrides and examine their structure as a function of composition as an important step toward developing chemical looping NH_3 production.

Ternary Nitride Down-Selection. Metal nitrides for the two-step chemical looping NH_3 production must meet a number of criteria. Radioactive, scarce, carcinogenic, or toxic constituents are undesirable and should be avoided. The materials must repeatedly release and reincorporate nitrogen without substantial or irreversible physical and chemical degradation. Moreover, above all, the construct of the thermochemical cycle must be thermodynamically plausible.

We began by considering binary nitrides (MN) from a thermodynamic perspective. The conventional construction of a thermochemical cycle relies on the additive nature of chemical reactions and the associated reaction thermodynamics, wherein two reactions that are more favorable replace one thermodynamically unfavorable reaction. Figure 2a presents an idealized case for the thermochemical cycle. The forthcoming discussions for Gibbs free energy, enthalpy, and entropy changes are averaged over the temperature range of interest, 273−1273 K, at 1 bar. The black line is the H−B reaction and is also indicative of ammonia stability. In this scenario, the ammonia formation from the nitride (blue) is favorable (negative ΔG) at temperatures > 977 K (shaded area on right of Figure 2a) and is mildly endothermic ($\Delta H \approx 105$ kJ mol^{-1}; $\Delta H = \Delta G + T\Delta S$). Ideally, the favorable region occurs at the lowest possible temperature to avoid spontaneous NH_3 decomposition. As the reactions are linked and must sum to the ammonia synthesis (black line), the corresponding nitridation reaction (red) must be exothermic, in the case shown as $\Delta H = -209$ kJ mol^{-1}, and thermodynamically favorable at any temperature below the intersection of the blue and black lines (shaded area on the left). In contrast to the ammonia formation reaction, it is preferable for the favorable nitridation reaction to occur at temperatures as high as possible to enhance reaction kinetics, as the strong N_2 triple bonds must be broken, and nitrogen must presumably diffuse into and throughout the solid nitride.

The free energy change (ΔG) of the reaction can be manipulated toward these aims either through the entropy (ΔS) or enthalpy (ΔH). Regarding entropy change (the slopes in Figure 2a), the $-\Delta S$ of the standard ammonia synthesis reaction is large (ca. -224 J mol^{-1} K^{-1}). In order for the ΔG line for the nitridation reaction to intersect that of the standard reaction, its $-\Delta S$ must be larger than the standard reaction and its ΔH more exothermic. That is, the slope of the red line must be greater than the slope of the black line, as depicted in Figure 2a. Figure 2b illustrates the thermodynamics of nitridation for numerous binary nitrides. Reviewing the data for binary nitrides in this context (albeit from the metals, Figure 2b), we make several significant observations. First, the positive slopes justify the arbitrary choice of the red line in Figure 2a as representing nitridation. Second, the observed ΔS values for nitridation show very little variation with regard to the choice of metal cation. One might anticipate this result, as the loss of gas phase N_2, as it reacts, accounts for most of the entropy change and is independent of a given metal. Finally, the ΔS values are unfortunately similar to the ΔS of the ammonia synthesis reaction, and to the extent that they do vary, the

https://doi.org/10.1021/acs.chemmater.3c00606
Chem. Mater. XXXX, XXX, XXX−XXX

variation tends toward ΔS being smaller rather than larger than the ΔS for the H−B reaction. This suggests that the ideal situation presented in Figure 2a may be difficult to replicate and also that the ability to alter the ΔS for nitridation, i.e., increasing the slope to engineer intersections in ΔG plots, through compound formation and substitution or doping, is likely to be limited. However, creating an ideal cycle is not an absolute requirement as other considerations such as operating conditions also play a role.

In contrast to ΔS, the ΔH for nitride regeneration varies over a range of at least 600 kJ mol^{-1}. Importantly, the range of data in Figure 2b includes binary examples where nitride formation is not favorable at any temperatures of interest (273−1273 K) and the reaction enthalpy ($\Delta H = \Delta G$ at $T = 0$ K) is greater than that of the H−B reaction. This group includes metals such as Fe, Co, Ni, Zn, and In, which we classify as A-group metals. In contrast, there is another group where nitride formation is favorable at almost all temperatures of interest, and the reaction enthalpy is more exothermic than the H−B reaction. The latter group, including metals such as Mo, W, Mn, Cr, and Ga, is classified as B-group metals. This observation suggests that reaction enthalpies may be highly tunable through combinations of metals between the two groups to form ternary nitrides and potentially provide a powerful route to cycle optimization. Nevertheless, given the inherent thermodynamic coupling of ammonia formation and nitride regeneration discussed above, it is expected that the principal metallic components will be drawn from those whose thermodynamics fall within a relatively narrow range around the conventional ammonia synthesis reaction ($\Delta H = -103.3$ kJ mol^{-1}, $\Delta G = -187$ to -38 kJ mol^{-1} for 273−1273 K). For the A-group metals mentioned previously, combinations with B-group metals may potentially yield nitride formation energies in this range.

However, this initial candidate consideration does not rule out the inclusion of other elements, particularly as minor constituents to modify the thermodynamics and/or promote the reaction kinetics.

To identify a suitable set of ternary nitrides (ABN) to meet the thermodynamic criteria above, we conducted an exhaustive down-selection from the periodic table. Figure 3 illustrates the down-selection process, using data from the Materials Project database.[27] Starting from the top in Figure 3a, all elements that were radioactive, scarce, non-metallic, or toxic were eliminated, leaving 41 elements. The nitride formation energy for MN binaries, where M was one of the remaining 41 elements, drove further down-selection. According to the construct in Figure 2, the ternary nitride should bind the nitrogen moderately more strongly than the bonds in ammonia. That is, the enthalpy of the ternary should be more negative than that of ammonia synthesis (ca. −46 kJ mol$_N^{-1}$ at 298 K). Thus, we reason the ternary should be constructed of those elements whose binary nitride reactions fall within a reasonable range around the ammonia synthesis reaction. We set the enthalpy range for the binary nitride formation from −180 kJ mol$_N^{-1}$ (relative to the H−B reaction), which eliminates 20 elements as binding to N is too strong, to 120 kJ mol$_N^{-1}$ (also relative to the H−B reaction), which eliminates another 3 as binding is too weak, leaving a total of 18. Figure 3b shows the remaining 18 elements divided into two groups: more favorable (columns) and less favorable (rows) formation enthalpies compared to NH_3 synthesis. (Fe is included in both categories as is it is only slightly more exothermic than H−B and is a known H−B catalysts that forms ternaries with other elements that bind N more strongly than ammonia.) It was reasoned that the combinations of these would yield ternaries with enthalpies intermediate to the binaries, i.e., balancing contributions from each metal. Each of those categories were further divided into those whose cations were redox-active (have multiple valence states) and those that were not. After the screening process, illustrated and described in Figure 3b, 47 potential candidates remained (green and dark green). The 22 dark green squares represent questionable candidates as they may bind with nitrogen too favorably or too unfavorably relative to NH_3. Eliminating these left 25 remaining candidates (light green boxes). The option of incorporating non-metals was re-examined at this point but resulted in no additional candidates (see Supporting Information). While the down-select did not take into consideration all parameters (e.g., entropy, range of possible operating conditions, etc.), it represents a practical

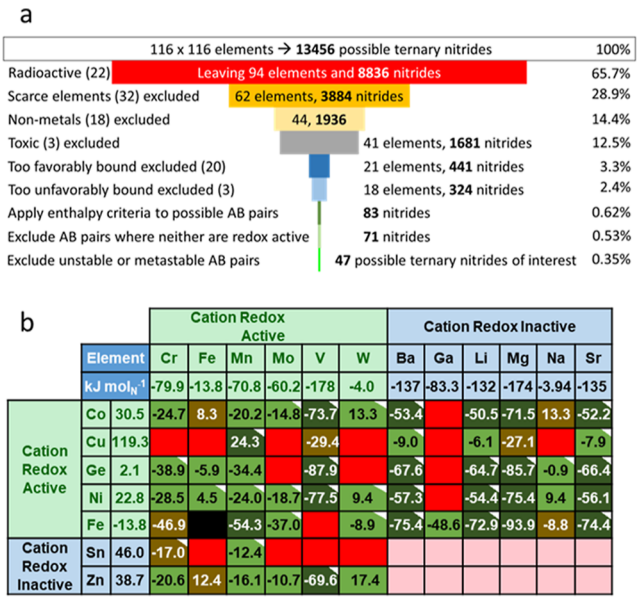

Figure 3. For a total space of 13,456 possible ternary nitrides: (a) Diagram depicting the down-selection process. Integers in parentheses correspond to the number of elements eliminated with each criterion. The percentages reflect the fraction of remaining possible ternary nitrides for each step compared to the entire space. (b) Down-selection from the final 18 elements. Elements are sorted into rows and columns based on the formation energy, relative to the H−B reaction, of the most stable binary found in the Materials Project database that has also been experimentally observed. Fe is included in both categories as is it is only slightly more exothermic than H−B, i.e., similar to the target metric, is known to form ternaries with elements from both groups, and is a known H−B catalyst. The intersections of rows and columns show average enthalpy values of the two binaries and represent an initial estimate for the ternary. Ternaries without at least one redox-active cation element are eliminated (pink boxes). Red boxes denote those eliminated as they are without predicted stable or metastable ternaries. Brown boxes denote those with predicted metastable ternaries (formation energies > 0.1 eV/atom, <0.2 eV/atom above the convex hull) but no predicted stable ternaries (formation energies ≤ 0.1 eV/atom above the convex hull). Of the remaining ternaries (47), 22 have either too favorable (21) or too unfavorable (1) binary reaction enthalpies (dark green). The 25 light green boxes denote the final down-selected candidates. White corners on the boxes indicate that a ternary nitride with that element pair has been experimentally observed. Data from Materials Project is current as of 10/10/2022.

https://doi.org/10.1021/acs.chemmater.3c00606
Chem. Mater. XXXX, XXX, XXX−XXX

starting pool of candidates to screen for chemical looping capability.

Next, we conducted a nitride synthesis campaign. The objective was to determine whether a sufficient pool of single-phase ternary and co-substituted quaternary candidate nitrides could be produced via facile synthesis methods to support validation of the approach and subsequent chemical looping development. To simplify the initial synthesis attempts, we excluded compositions with Sn, Zn, Cu, Ge, Ba, Li, Mg, Na, and Sr from the remaining candidates due to the potential for these metals to volatilize or melt at anticipated synthesis temperatures. However, we do not mean to imply that these should be categorically ruled out, as nitrides containing these elements might be obtainable by solvothermal or other alternative synthesis methods.[28,29] We selected Fe, Co, Ni for the A-group metals and Mo, W, and Mn for the B-group metals to synthesize a family of ternary and quaternary nitrides. The importance of co-substituted quaternaries lies in the potential to finely tune crystallite lattice parameters and formation energies to optimize the looping cycle as necessary. Mn-based compositions attempted using the synthesis method below,[30] yielded mixtures of metallic, alloy, or binary nitride phases in the final product with no indication of Mn-based ternary nitrides, thus Mn was excluded from further study.

The selection process carried out above identified a group of ternary compounds to target for synthesis and characterization. Of that group identified above as potential materials, Co_3Mo_3N was identified as being of particular interest, as it was reported in the literature that this material undergoes a complete and reversible transition to Co_6Mo_6N, resulting in a 50 mol % loss of nitrogen (eqs 1 and 2).[15,31−33] Further, it was reported that the lattice nitrogen in the material is mobile and that the material can be re-nitridized using pure N_2 gas, making it an attractive candidate.

EXPERIMENTAL SECTION

Two-Step Nitride Synthesis. Typically, Co_3Mo_3N and similar compounds are synthesized via a multi-step ammonolysis procedure that utilizes NH_3 or high concentrations of NH_3 with H_2 (up to 75%).[12,32−35] Several synthesis methods to make ternary and quaternary nitride materials described below were attempted before one was found that produced single phase samples of the desired stoichiometry.

The "urea glass" method, which has been reported for the synthesis of binary nitrides, including those of Mo, W, Co, Cr, and Ti, was first attempted. The process involves the dissolution of a metal precursor (often chloride) in ethanol, followed by addition of urea to form a gel, drying and calcining at 973−1073 K under flowing N_2.[36,37] We successfully synthesized Mo_2N via this method, but were unable to obtain any ternary nitrides.

We then attempted to synthesize Co_3Mo_3N via direct nitridation of metallic precursors.[38] Stoichiometric amounts of Co and Mo powders were ground with a mortar and pestle, transferred to a tube furnace, and heated to 1058 K under an atmosphere of 10% H_2 balanced with N_2 flow (10% H_2/N_2) at 100 sccm and 1 atm for 24 h. The materials were re-ground every 24 h. After 4 to 5 repetitions, we obtained ~85% of the target Co_3Mo_3N phase based on phase quantification in XRD and mass balances. The remaining 15% included a Co_2Mo_3N phase and small amounts of Mo_2N and Mo−Co alloy phases.

To improve synthesis efficiency and outcomes, we next adopted a two-step method, which was also found to be effective for synthesizing quaternary nitrides, including $(Co,Fe)_3Mo_3N$, $(Fe,Ni)_2Mo_3N$, and $(Co,Ni)_2Mo_3N$. The first step is a modified Pechini method to prepare the oxide precursors.[15,39] In a typical synthesis, stoichiometric amounts (metals basis) of $(NH_4)_6Mo_7O_{24}\cdot 4H_2O$ (1.7655 g, Sigma-Aldrich, 81.0−83.0% MoO_3 basis), $Fe(NO_3)_3\cdot 9H_2O$ (Sigma-Aldrich, ≥98%), $Co(NO_3)_2\cdot 6H_2O$ (Sigma-Aldrich, ≥98%), and/or $Ni(NO_3)_2\cdot 6H_2O$ (Sigma-Aldrich, ≥99.999%) were dissolved in 100 mL deionized water at room temperature in a beaker. The target compositions for the nitrides are shown in Table 1. We then added citric acid monohydrate (Sigma-Aldrich, ≥99.0%) as a chelating agent. The typical molar ratio of metal (M) to citric acid (CA) was M/CA = 1:3. The mixture was stirred on a hotplate at 343 K for 30 min to obtain a transparent solution. The temperature was then raised to 393 K to promote evaporation. The stirring was halted at the onset

Table 1. Target Chemical Compositions and Abbreviations of the (Fe, Co, Ni)−Mo−N Nitrides and Their Lattice Parameters from X-ray Diffractometry Analysis[a]

target composition	abbreviation	lattice parameter a (Å)	crystallite size (nm)
Fe_3Mo_3N	FMN	10.99	126
Co_3Mo_3N	CMN	10.95	114
Ni_2Mo_3N	NiMN	6.57	129
$(Fe_{0.25}Co_{0.75})_3Mo_3N$	FCMN2575	10.95	82
$(Fe_{0.5}Co_{0.5})_3Mo_3N$	FCMN5050	10.97	111
$(Fe_{0.75}Co_{0.25})_3Mo_3N$	FCMN7525	10.99	82
$(Fe_{0.25}Ni_{0.75})_2Mo_3N$	FNiMN2575	6.60	65
$(Fe_{0.5}Ni_{0.5})_2Mo_3N$	FNiMN5050	6.60	35
$(Fe_{0.75}Ni_{0.25})_2Mo_3N$	FNiMN7525	6.62 for 231 phase	33 for 231 phase
		10.99 for 331 phase	95 for 331 phase
$(Co_{0.25}Ni_{0.75})_2Mo_3N$	CNiMN2575	6.58	56
$(Co_{0.5}Ni_{0.5})_2Mo_3N$	CNiMN5050	6.59	98
$(Co_{0.75}Ni_{0.25})_2Mo_3N$	CNiMN7525	6.61	68

[a]331 compounds crystalize in cubic space group $Fd\bar{3}m$, and 231 compounds crystalize in cubic space group $P4_132$. Crystallite sizes were calculated via Scherrer equation. fwhm was determined from peaks on the (422), (511), and (440) planes for the 331 structures, and from peaks on the (221), (310), and (311) planes for the 231 structures.

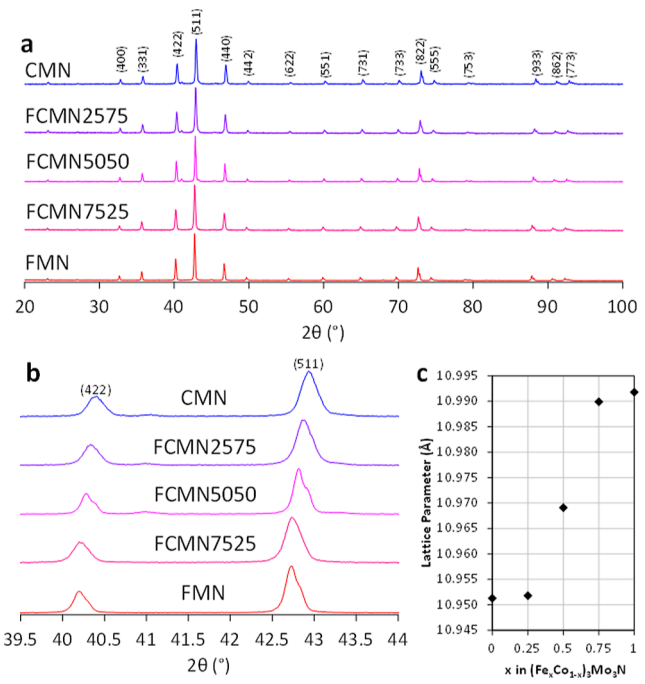

Figure 4. XRD patterns of the (Fe, Co)−Mo−N nitrides after synthesis. (a) Reflections in the 20−100° 2θ range. (b) Reflections in the 39.5−44° 2θ range. (c) Lattice parameter as a function of Fe content.

https://doi.org/10.1021/acs.chemmater.3c00606
Chem. Mater. XXXX, XXX, XXX−XXX

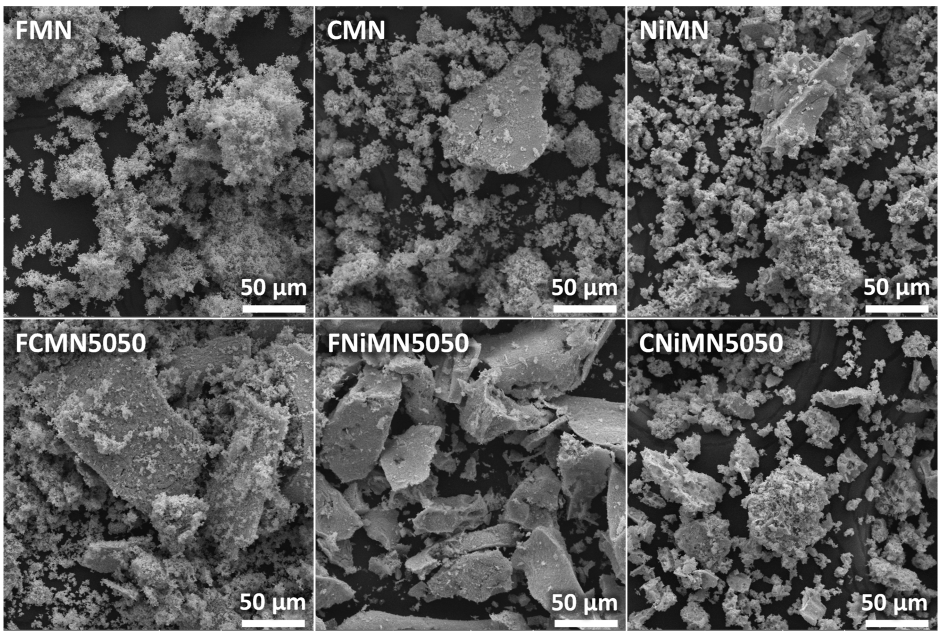

Figure 5. SEM images showing the agglomerates of as-synthesized FMN, CMN, NiMN, FCMN5050, FNiMN5050, and CNiMN5050 in a 0.25 mm view field.

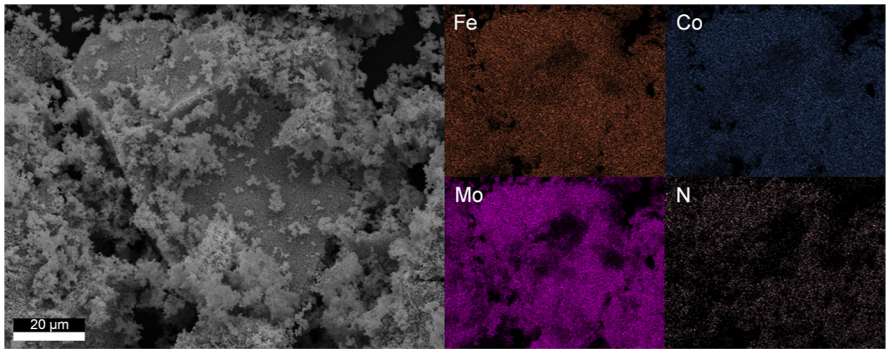

Figure 6. SEM image of FCMN5050 and its elemental distribution of Fe, Co, Mo, and N from energy dispersive X-ray spectroscopy.

of gel formation. At this time, depending on the majority composition of metallic ions in the mixture, the gel would be transparent orange (Fe majority), wine-red (Co majority), or green (Ni majority) in color. The beaker containing the gel was transferred to a drying oven to dehydrate for 15 h at 423 K, whereupon the gel expanded into a porous char-black monolithic foam. The monolith was crushed and finely ground before being transferred into an alumina crucible and calcined in air in a box furnace at 823 K for 6 h. The as-synthesized oxide precursors after calcination were brown (Fe majority), violet (Co majority), or green (Ni majority) in color. The crushing and grinding process proved important as attempts with only consecutive dehydration (423 K) and calcination (823 K) resulted in oxide precursors that required more than double the dwell time in the subsequent nitridation step to convert into near single-phase nitrides.

Samples of 0.5 to 10 mol % (in 0.5 mol % increments) Ni- (A-group) or W (B-group) -substituted $CoMoO_4$ precursors were synthesized via the same modified Pechini method in a 1:1 A/B metals ratio, using a $(NH_4)_{10}H_2(W_2O_7)_6$ (Sigma-Aldrich, ≥99.99%) precursor in the case of W-substitution.

In the final step, the oxide precursors were converted into nitrides following a nitridation procedure reported by Hunter et al.,[15] with modifications. Approximately 250 mg of oxide precursor were loaded as a 1 mm thin layer in an alumina boat, transferred into a quartz tube reactor (20 mm ID), and nitridated under 50 sccm of H_2/N_2 mixture (10% H_2 with N_2 balance, Linde). The heating profile was: (i) ambient temperature to 630 K at a rate of 5.6 K·min^{-1}, (ii) 630−720 K at a rate of 0.5 K·min^{-1}, and (iii) 720−1073 K at a rate of 2.1 K·min^{-1}, then held for 12 h at 1073 K. The sample was subsequently cooled to room temperature via a cooling ramp that was the reverse of the heating ramp.

Characterization. Sample phase and purity was determined via powder X-ray diffractometry (XRD, Malvern PANalytical Aeris, Cu Kα radiation). Measurements were taken in the 5−110° 2θ range with a step size of 0.01°. XRD patterns were matched to entries in the ICDD PDF-4+ database. Whole pattern fitting using JADE provided lattice parameter and crystallite size data.[40]

Sample morphology and elemental distribution were analyzed via scanning electron microscopy (SEM, TESCAN Vega3) with energy dispersive X-ray spectroscopy (EDX, EDAX Element X1). Samples were prepared on sample stubs with carbon tape and sputter-coated with Au/Pd (Denton Vacuum Desk IV) for ∼30 s at 37% power to prevent sample charging. SEM was performed at multiple locations on each sample using an accelerating voltage of 20 kV, with corresponding EDX elemental maps produced at a working distance of approximately 15 mm for each area. Magnification and working distance were selected to characterize the samples at the particle bed and particle surface level to qualitatively evaluate particle morphology.

Preliminary screening of Co_3Mo_3N for reduction and re-nitridation was performed via thermogravimetric analysis (TGA, TA Instruments Q600). The experimental parameters and results are summarized in Supporting Information.

https://doi.org/10.1021/acs.chemmater.3c00606
Chem. Mater. XXXX, XXX, XXX−XXX

RESULTS AND DISCUSSION

Structural Characterization of Nitrides. To determine co-substitution limits in the (Fe, Co, Ni)−Mo−N nitride solid solutions, we synthesized a series of ternary and quaternary nitrides. Table 1 summarizes target compositions and their abbreviations. Preliminary synthesis efforts suggested that compositions containing Ni crystallized in the filled β-manganese phase, labelled as 231. Therefore, to achieve >95% single phase in the final nitride samples, all target compositions with >25 mol % Ni A-group occupancy used precursor input ratios suitable for the 231 phase. All target compositions without Ni used precursor input ratios to achieve the η-carbide phase, labelled as 331.

Figure 4 shows XRD patterns of the (Fe, Co)−Mo−N ternary and quaternary nitrides, all of which crystallized in the $Fd\bar{3}m$ space group (PDF 01-077-8334 Fe_3Mo_3N, 01-080-3329 Co_3Mo_3N). A small secondary phase appears in samples with ≥50 mol % Co content, indicated by reflections at ca. 41.06 and 43.29°, corresponding to the Co_2Mo_3N phase. These secondary phases account for less than 5% according to quantitative phase analysis. The secondary phase was undetectable by XRD for subsequent samples subjected to longer (>24 h) nitridation times. However, for consistency of synthesis conditions, only CMN samples prepared with 12 h nitridation times are included in comparisons with Fe and Ni counterparts. Within this context, combinations of Fe and Co in the A group appear to be completely miscible, i.e., capable of forming a single 331 phase, independent of Co/Fe ratio. A small peak shift toward higher 2θ was observed with increasing Co content, indicative of lattice contraction as Co substitutes for Fe. A magnified view of peak shifts on the (422) and (511) planes is shown in Figure 4b. The lattice parameters derived from whole pattern fitting are shown in Figure 4c and are summarized in Table 1. These results of lattice parameters are consistent with reported data, where ternary nitrides were prepared from ammonolysis of oxide precursors prepared by

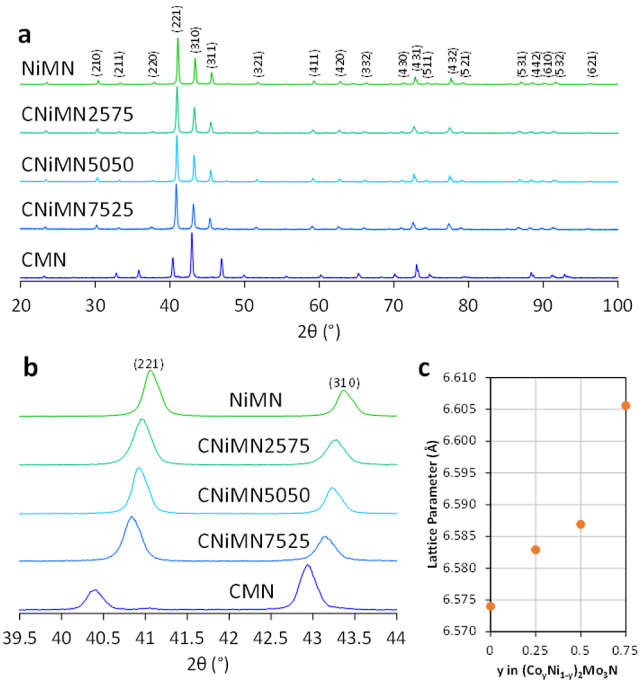

Figure 7. XRD patterns of the (Co, Ni)−Mo−N nitrides after synthesis. (a) Reflections in the 20−100° 2θ range. (b) Reflections in the 39.5−44° 2θ range. (c) Lattice parameter as a function of Co content.

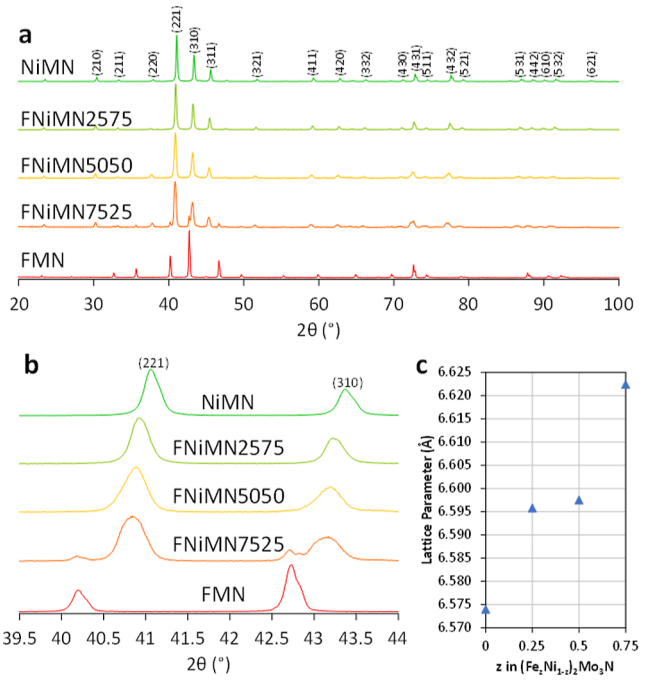

Figure 9. XRD patterns of the (Fe, Ni)−Mo−N nitrides after synthesis. (a) Reflections in the 20−100° 2θ range. (b) Reflections in the 39.5−44° 2θ range. (c) Lattice parameter as a function of Fe content.

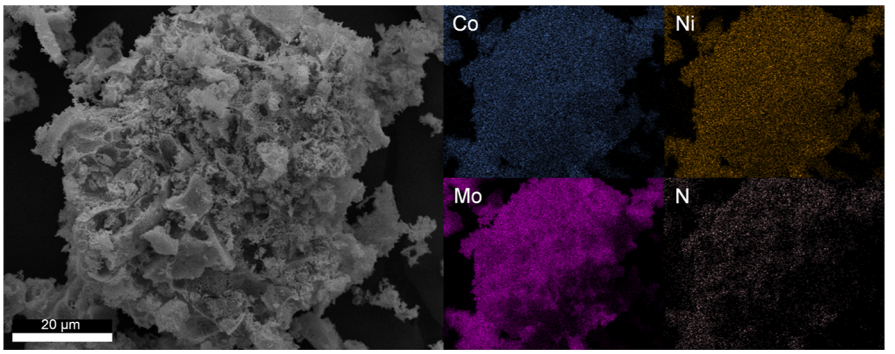

Figure 8. SEM image of CNiMN5050 and its elemental distribution of Co, Ni, Mo, and N from energy dispersive X-ray spectroscopy.

https://doi.org/10.1021/acs.chemmater.3c00606
Chem. Mater. XXXX, XXX, XXX−XXX

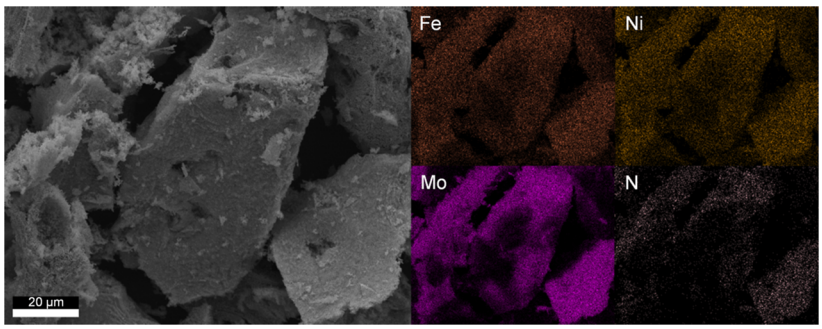

Figure 10. SEM image of FNiMN5050 and its elemental distribution of Fe, Ni, Mo, and N from energy dispersive X-ray spectroscopy.

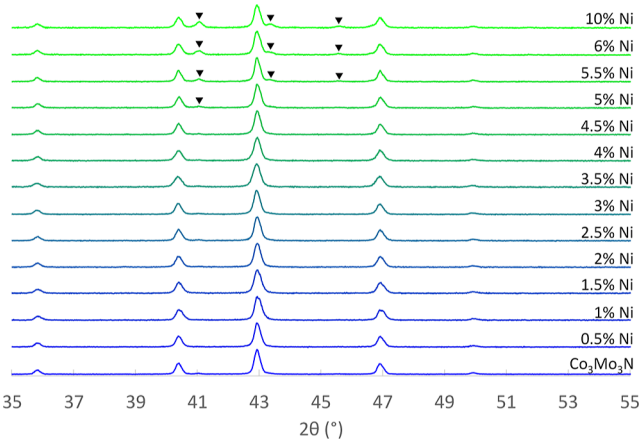

Figure 11. XRD patterns of the low content nickel A-group substituted $(Ni_xCo_{1-x})_3Mo_3N$ nitrides. Samples were prepared with 0.5% increments of Ni content, up to 10%. Black triangles mark the secondary 231 phase.

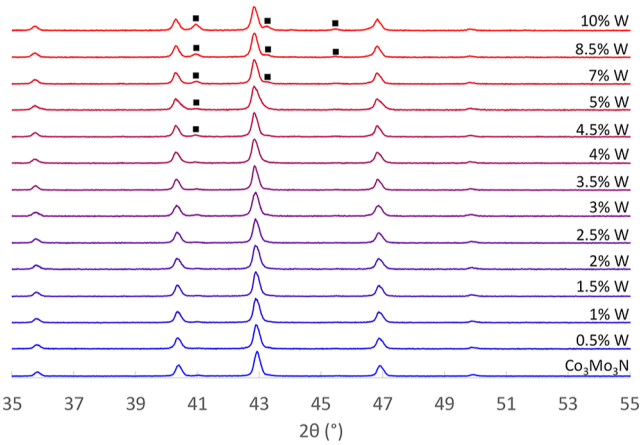

Figure 12. XRD patterns of the low content tungsten B-group substituted $Co_3(W_xMo_{1-x})_3N$ nitrides. Samples were prepared with 0.5% increments of W content, up to 10%. Black squares mark the secondary 231 phase.

co- precipitation (a = 11.0859 Å for Fe_3Mo_3N, and a = 11.0270 Å for Co_3Mo_3N).[41,42]

The progressive shift in the lattice parameters indicates the potential to tune bond distances within the ternary nitride structures, potentially unlocking a tunable pair of reactions in the intended chemical looping scheme. Notice the shift in lattice parameters do not obey the linear relationship dictated by the Vegard's law and is subject to further investigation.[43,44]

Representative SEM images of FMN, CMN, and FCMN5050 are shown in Figure 5. All samples were mixtures of larger agglomerates decorated by smaller microparticles. Figure 6 shows the EDX elemental distribution of FCMN5050. The uniform distribution of Fe, Co, Mo, and N, immaterial of particle size or morphology and without any apparent elemental segregation, is consistent with the predominantly 331 phase in the XRD analysis.

Figure 7a,b shows XRD patterns of the (Co, Ni)−Mo−N ternary and quaternary nitrides. All quaternary compositions and NiMN yielded 231 nitrides consistent with the ratios used during synthesis, with minimum indication of secondary impurities. In contrast, the pattern for CMN is consistent with the 331 structure and the starting metal stoichiometry in the synthesis. The calculated lattice parameters (Table 1) agree with reported NiMN data (a = 6.6342 Å for Ni_2Mo_3N)[42] and increase with increasing Co content (Figure 7c). Figure 5 shows corresponding SEM images of CMN, NiMN, and CNiMN5050, and Figure 8 shows a higher magnification SEM and EDX examination of CNiMN5050. The predominant morphology is faceted agglomerates of ca. 10 μm. EDX shows a uniform elemental distribution of Co, Ni, Mo, and N, again in agreement with the single-phase analysis from XRD results.

We also synthesized and characterized (Fe, Ni)−Mo−N nitrides (Figure 9). Increasing substitution of Fe for Ni resulted in XRD peak broadening in the 231 structure, indicating a decreasing trend of crystallite size for this structure (Table 1). A single phase persists up to 50 mol % Fe. At 75 mol % Fe, however, an apparent secondary 331 phase segregates from the majority 231 phase, indicating the substitution limit was exceeded. Apart from crystallite size effects, the increased reflection peak broadening with increasing Fe-substitution may also be attributed to structural disorder effects.[54,55] The evident non-uniform peak broadening observed in FNiMN5050 is particularly an indication of structural disorder, possibly an indication of the nitride approaching its substitution limit. Figure 9c shows the lattice parameter increases with increasing Fe content within the 231 structure. In FNiMN5050, SEM (Figure 10) shows agglomerates similar to the faceted morphology of NiMN, but much larger in size at ca. 50−100 μm. Elemental EDX mapping shows a uniform distribution of Fe, Ni, Mo, and N elements in FNiMN5050, in agreement with the single 231 phase seen in XRD.

The synthesis study demonstrates the existence of a wide stability window for substituted nitrides in the family of (Fe, Co, Ni)−Mo−N, enabling the potential fine tuning of nitride properties for chemical looping NH_3 synthesis. Note that the stoichiometric FMN, CMN, and NiMN nitrides are known

https://doi.org/10.1021/acs.chemmater.3c00606
Chem. Mater. XXXX, XXX, XXX−XXX

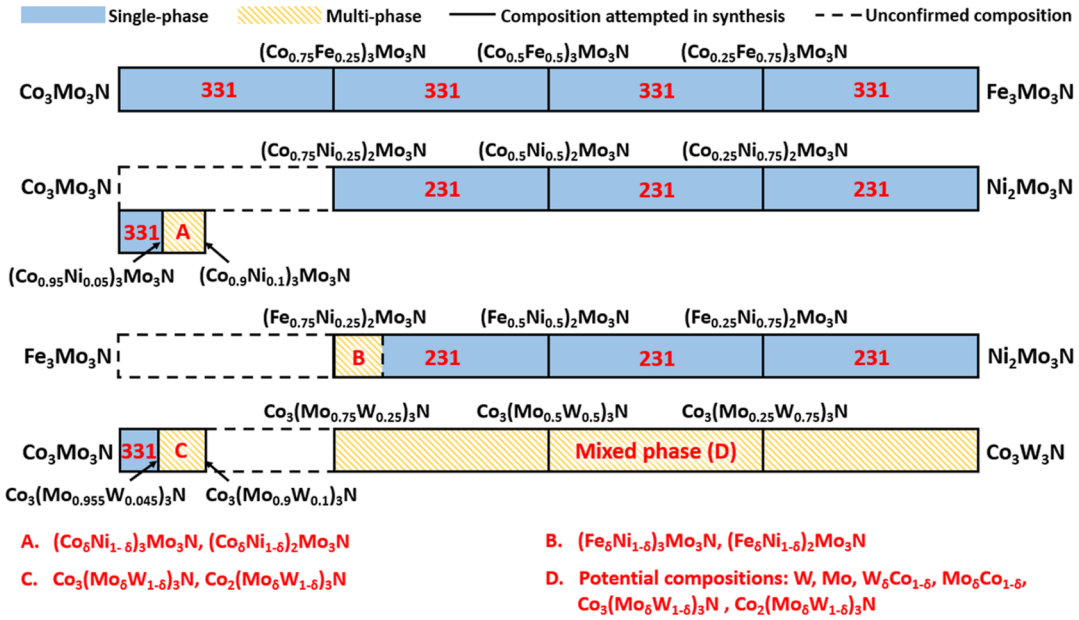

Figure 13. Phase stability of ABN (A = Co, Fe, Ni; B = Mo, W) nitrides. The synthesis precursors were metal oxides prepared by a modified Pechini method. The precursors were then nitridized with a 10% H_2/N_2 mixture gas (50 sccm) at up to 1073 K for 12 h to obtain the nitrides. 331: η-carbide structure; 231: filled β-manganese structure.

NH_3 synthesis catalysts, and similar bi-metallic systems are often of interest to catalyst scientists.[45−48] This is because the ability of catalyst constituents to cycle between oxidation states (donate and accept electrons) is crucial to many catalytic processes, and the ability to manipulate the thermodynamics/bond strengths of those redox processes by mixing metals is an important tool available to scientists seeking to manipulate or optimize the material. For specific examples, consider that Perret et al., reported in a H_2 chemisorption and temperature programmed desorption experiment that bi-metallic CMN and FMN compounds demonstrated 4−8 times higher H_2 release compared to mono-metallic Mo_2N, and linked the results to the observation of more nitrogen-deficient sites in the bi-metallic nitride compounds.[45] Wang et al., demonstrated that an optimal loading of 1 wt % $Ni_{0.2}Mo_{0.8}N$ with In_2S_3 resulted in 10 times higher photocatalytic H_2 production rate than that of pure In_2S_3 and described the $Ni_{0.2}Mo_{0.8}N$ as possessing metallic-like properties that facilitate electron transfer from In_2S_3.[46] The improved catalytic activity of the ternary nitrides is generally associated with their dominant metal−metal interactions and the interstitial N atoms within the metal array.[45] Despite these examples, the capability to efficiently and reversibly access the N atoms in these ternaries for NH_3 synthesis requires further in-depth study.

Earlier reports suggest the Ni-based 231-structured nitride is a stable phase under reduction conditions and disputed the existence of a Ni_3Mo_3N compound.[38] However, no studies have determined definitively whether a stable 331 nitride with a given Ni-substitution fraction can be synthesized. Our work with nitridation of Pechini oxide precursors suggests such substitution is unlikely to be achieved with >25 mol % Ni-substituted in the A group. To determine Ni-substitution limit in the 331 structure, we investigated low-concentration Ni-substitution into CMN from 0.5 to 10 mol %, in 0.5 mol % increments. Figure 11 shows XRD patterns of the as-prepared $(Ni_xCo_{1-x})_3Mo_3N$ nitrides. Phase quantification suggests that >95% 331 phase exists up to 5 mol % Ni, beyond which evidence of a 231 phase becomes apparent. Additionally, a shift of XRD peaks in the 331 phase toward higher diffraction angles with increasing Ni content is evident, indicating decreasing lattice parameter with increasing Ni content. The ability of Co_3Mo_3N to maintain the 331 structure while allowing low content substitution with Ni expands the possibilities for tuning 331 nitride thermodynamics.

The results demonstrate material tunability via A-group cation substitution. B-group cation substitutions could be equally beneficial. To date, examples of this are scarce, likely because they have proven difficult to synthesize.[29,30,49,50] One potential candidate to replace Mo as the B-group element is W (see Ternary Nitride Down-Selection). However, W-based ternaries require significantly more demanding synthesis conditions to achieve single phase solid solutions with a stable 331 phase.[49−53] Our preliminary attempts to synthesize Co_3W_3N via the nitridation of Pechini-derived $CoWO_4$ precursor with flowing 10% H_2/N_2 yielded metallic W and Co−W alloy mixtures with no indication of nitride formation despite multiple attempts in which the holding temperature was varied over the range of 823−1173 K. However, upon substituting W with increasing amounts of Mo, a trend of ternary nitride formation began to appear. At 75 mol % Mo and 25 mol % W, metallic (W or Mo) or alloy (Co−W or Co−Mo) phases were no longer detected in the post-synthesis XRD. Still, the resulting nitrides were a mixture of 331 and 231 phases. To investigate the limits in which a single 331 phase of $Co_3(W_xMo_{1-x})_3N$ can be obtained, we substituted W for Mo in Co_3Mo_3N in 0.5% increments. The XRD patterns of the as-prepared nitrides are shown in Figure 12. Similar to the case of Co_3Mo_3N with A-group substitution by Ni, a secondary 231 phase appeared in $Co_3(W_xMo_{1-x})_3N$ with increasing W content. Also similar, for W-substitution below 4.5 mol %, a majority (>95% by XRD) 331 phase was present. In the secondary phases, we did not observe W, W−Mo, or W nitrides (W_2N, WN, WN_2) that would indicate W precipitation or segregation. A shift of the 331 diffraction peaks toward

https://doi.org/10.1021/acs.chemmater.3c00606
Chem. Mater. XXXX, XXX, XXX−XXX

lower angles (lattice expansion) with increasing W content confirms the increasing incorporation of W into the lattice. While the demonstrated W-substitution window is narrow, it broadens the ternary nitride material tunability to the B-group and expands the range of possibilities for tunability of nitrogen activity. As a summary, the phase stability of the ABN (A = Co, Fe, Ni; B = Mo, W) nitride system based on the initial synthesis composition is shown in Figure 13.

Our preliminary screening of Co_3Mo_3N via TGA studies suggested promising NH_3 synthesis capabilities via chemical looping and is summarized in Supporting Information. Reduction of Co_3Mo_3N in 75% H_2/Ar mixture resulted in trace amount of NH_3 production verified by mass spectrometry and a H_2SO_4 indicator, as described by Shaw and Staddon,[56] confirming the ability for nitrogen removal in Co_3Mo_3N. The observed mass loss of ~1.5 wt % is consistent with the theoretical mass loss of 1.46 wt % when converting Co_3Mo_3N to Co_6Mo_6N. Subsequent studies of thermochemical cycles for NH_3 production using the Co_3Mo_3N/Co_6Mo_6N pair have confirmed the reversible nitrogen removal/uptake activity, and the associated manuscript is currently under review.

CONCLUSIONS

We have proposed that a new two-step chemical looping pathway may be a competitive alternative to the conventional H−B process for NH_3 production by mitigating thermodynamic and kinetics conflicts. We have systematically evaluated the periodic table to identify elemental candidates for ABN ternary nitrides potentially capable of NH_3 production and nitride regeneration reactions under reasonable conditions. From this screening process, we selected Fe, Co, and Ni for the A-group metals, and Mo and W for the B-group metals, as examples to construct a pool of ternary and quaternary nitrides for experimental evaluation. We successfully synthesized over 30 materials from this family via a facile two-step synthesis method and characterized their phase, lattice parameter, crystallite size, morphology, homogeneity, and miscibility limits. Our study suggests a possible wide range of solid-state miscibility exists for the (Fe, Co, Ni)−(Mo, W)−N system, in both the 331 and 231 phases. Additional work to evaluate these versatile nitrides in the chemical looping mechanism to produce NH_3 is ongoing.

ASSOCIATED CONTENT

Supporting Information

The Supporting Information is available free of charge at https://pubs.acs.org/doi/10.1021/acs.chemmater.3c00606.

Ternary nitride down-selection with non-metals and Co_3Mo_3N sample screening (PDF)

AUTHOR INFORMATION

Corresponding Author

Ellen B. Stechel − *ASU LightWorks, Arizona State University, Tempe, Arizona 85287-8204, United States; School of Molecular Sciences, Arizona State University, Tempe, Arizona 85287-8204, United States;* orcid.org/0000-0002-5379-2908; Email: ellen.stechel@asu.edu

Authors

Xiang Gao − *ASU LightWorks, Arizona State University, Tempe, Arizona 85287-8204, United States;* orcid.org/0009-0009-4894-4071

H. Evan Bush − *Concentrating Solar Technologies, Sandia National Laboratories, Albuquerque, New Mexico 87185-1127, United States;* orcid.org/0000-0002-8305-9344

James E Miller − *ASU LightWorks, Arizona State University, Tempe, Arizona 85287-8204, United States; School of Sustainability, Arizona State University, Tempe, Arizona 85287-8204, United States*

Alicia Bayon − *ASU LightWorks, Arizona State University, Tempe, Arizona 85287-8204, United States; Instituto de Catálisis y Petroleoquímica (CSIC), Madrid 28049, Spain*

Ivan Ermanoski − *ASU LightWorks, Arizona State University, Tempe, Arizona 85287-8204, United States; School of Sustainability, Arizona State University, Tempe, Arizona 85287-8204, United States*

Andrea Ambrosini − *Concentrating Solar Technologies, Sandia National Laboratories, Albuquerque, New Mexico 87185-1127, United States*

Complete contact information is available at: https://pubs.acs.org/10.1021/acs.chemmater.3c00606

Notes

The authors declare no competing financial interest.

ACKNOWLEDGMENTS

This material is based on work supported by the U.S. Department of Energy under award no. DE-EE0034250. The authors wish to acknowledge the team and institutions involved in this work: Arizona State University, Sandia National Laboratories, and Georgia Institute of Technology. The assistance in nitride synthesis by Nathaniel Anbar, Syed Shakeel, and Jarett Prince is also greatly acknowledged. We gratefully acknowledge the use of facilities within the Eyring Materials Center at Arizona State University supported in part by NNCI-ECCS-1542160, and in particular David Wright for his above-and-beyond help and support with our first successful nitride synthesis. This article has been authored by an employee of National Technology & Engineering Solutions of Sandia, LLC under Contract No. DE-NA0003525 with the U.S. Department of Energy (DOE). The employee owns all right, title and interest in and to the article and is solely responsible for its contents. The United States Government retains and the publisher, by accepting the article for publication, acknowledges that the United States Government retains a non-exclusive, paid-up, irrevocable, world-wide license to publish or reproduce the published form of this article or allow others to do so, for United States Government purposes. The DOE will provide public access to these results of federally sponsored research in accordance with the DOE Public Access Plan https://www.energy.gov/downloads/doe-public-access-plan. This paper describes objective technical results and analysis. Any subjective views or opinions that might be expressed in the paper do not necessarily represent the views of the U.S. Department of Energy or the United States Government.

REFERENCES

(1) Ertl, G. Primary Steps in Catalytic Synthesis of Ammonia. *J. Vac. Sci. Technol., A* **1983**, *1*, 1247−1253.

(2) Tanabe, Y.; Nishibayashi, Y. Developing More Sustainable Processes for Ammonia Synthesis. *Coord. Chem. Rev.* **2013**, *257*, 2551−2564.

(3) Hessel, V.; Anastasopoulou, A.; Wang, Q.; Kolb, G.; Lang, J. Energy, Catalyst and Reactor Considerations for (near)-Industrial

Plasma Processing and Learning for Nitrogen-Fixation Reactions. *Catal. Today* **2013**, *211*, 9−28.
(4) Bazhenova, T. A.; Shilov, A. E. Nitrogen Fixation in Solution. *Coord. Chem. Rev.* **1995**, *144*, 69−145.
(5) Peters, J. W.; Szilagyi, R. K. Exploring New Frontiers of Nitrogenase Structure and Mechanism. *Curr. Opin. Chem. Biol.* **2006**, *10*, 101−108.
(6) Anderson, J. S.; Rittle, J.; Peters, J. C. Catalytic Conversion of Nitrogen to Ammonia by an Iron Model Complex. *Nature* **2013**, *501*, 84−87.
(7) Arashiba, K.; Miyake, Y.; Nishibayashi, Y. A Molybdenum Complex Bearing PNP-Type Pincer Ligands Leads to the Catalytic Reduction of Dinitrogen into Ammonia. *Nat. Chem.* **2011**, *3*, 120−125.
(8) Michalsky, R.; Pfromm, P. H. Chromium as Reactant for Solar Thermochemical Synthesis of Ammonia from Steam, Nitrogen, and Biomass at Atmospheric Pressure. *Sol. Energy* **2011**, *85*, 2642−2654.
(9) Michalsky, R.; Parman, B. J.; Amanor-Boadu, V.; Pfromm, P. H. Solar Thermochemical Production of Ammonia from Water, Air and Sunlight: Thermodynamic and Economic Analyses. *Energy* **2012**, *42*, 251−260.
(10) Michalsky, R.; Pfromm, P. H.; Steinfeld, A. Rational Design of Metal Nitride Redox Materials for Solar-Driven Ammonia Synthesis. *Interface Focus* **2015**, *5*, 20140084.
(11) Michalsky, R.; Avram, A. M.; Peterson, B. A.; Pfromm, P. H.; Peterson, A. A. Chemical Looping of Metal Nitride Catalysts: Low-Pressure Ammonia Synthesis for Energy Storage. *Chem. Sci.* **2015**, *6*, 3965−3974.
(12) Kojima, R.; Aika, K. Cobalt Molybdenum Bimetallic Nitride Catalysts for Ammonia Synthesis. *Appl. Catal., A* **2001**, *215*, 149−160.
(13) Kojima, R.; Aika, K. Cobalt Molybdenum Bimetallic Nitride Catalysts for Ammonia Synthesis. *Appl. Catal., A* **2001**, *218*, 121−128.
(14) Kojima, R.; Aika, K. Cobalt Molybdenum Bimetallic Nitride Catalysts for Ammonia Synthesis. *Appl. Catal., A* **2001**, *219*, 157−170.
(15) Gregory, D. H.; Hargreaves, J. S. J.; Hunter, S. M. On the Regeneration of Co_3Mo_3N from Co_6Mo_6N with N_2. *Catal. Lett.* **2011**, *141*, 22−26.
(16) Farr, T. P.; Nguyen, N. P.; Bush, H. E.; Ambrosini, A.; Loutzenhiser, P. G. An A- and B-Site Substitutional Study of $SrFeO_{3-\delta}$ Perovskites for Solar Thermochemical Air Separation. *Materials* **2020**, *13*, 5123.
(17) Bush, H. E.; Nguyen, N. P.; Farr, T.; Loutzenhiser, P. G.; Ambrosini, A. Air Separation via a Two-Step Solar Thermochemical Cycle Based on $(Ba,La)_XSr_{1-X}FeO_{3-\delta}$: Thermodynamic Analysis. *Solid State Ionics* **2021**, *368*, 115692.
(18) Nguyen, N. P.; Farr, T. P.; Bush, H. E.; Ambrosini, A.; Loutzenhiser, P. G. Air Separation via Two-Step Solar Thermochemical Cycles Based on $SrFeO_{3-\delta}$ and $(Ba,La)_{0.15}Sr_{0.85}FeO_{3-\delta}$ Perovskite Reduction/Oxidation Reactions to Produce N_2 : Rate Limiting Mechanism(s) Determination. *Phys. Chem. Chem. Phys.* **2021**, *23*, 19280−19288.
(19) Sun, W.; Bartel, C. J.; Arca, E.; Bauers, S. R.; Matthews, B.; Orvañanos, B.; Chen, B.-R.; Toney, M. F.; Schelhas, L. T.; Tumas, W.; Tate, J.; Zakutayev, A.; Lany, S.; Holder, A. M.; Ceder, G. A Map of the Inorganic Ternary Metal Nitrides. *Nat. Mater.* **2019**, *18*, 732−739.
(20) Marchand, R.; Laurent, Y.; Guyader, J.; L'Haridon, P.; Verdier, P. Nitrides and Oxynitrides: Preparation, Crystal Chemistry and Properties. *J. Eur. Ceram. Soc.* **1991**, *8*, 197−213.
(21) Sun, W.; Holder, A.; Orvañanos, B.; Arca, E.; Zakutayev, A.; Lany, S.; Ceder, G. Thermodynamic Routes to Novel Metastable Nitrogen-Rich Nitrides. *Chem. Mater.* **2017**, *29*, 6936−6946.
(22) Zakutayev, A.; Bauers, S. R.; Lany, S. Experimental Synthesis of Theoretically Predicted Multivalent Ternary Nitride Materials. *Chem. Mater.* **2022**, *34*, 1418−1438.
(23) Laassiri, S.; Zeinalipour-Yazdi, C. D.; Catlow, C. R. A.; Hargreaves, J. S. J. The Potential of Manganese Nitride Based Materials as Nitrogen Transfer Reagents for Nitrogen Chemical Looping. *Appl. Catal., B* **2018**, *223*, 60−66.
(24) Dinh, V. A.; Sato, K.; Katayama-Yoshida, H. Carrier Co-Doping Method with Size Compensation to Enhance TC of Mn-Doped Nitrides. *J. Supercond.* **2005**, *18*, 47−53.
(25) Gagné, O. C. On the Crystal Chemistry of Inorganic Nitrides: Crystal-Chemical Parameters, Bonding Behavior, and Opportunities in the Exploration of Their Compositional Space. *Chem. Sci.* **2021**, *12*, 4599−4622.
(26) Scott Weil, K.; Kumta, P. N.; Grins, J. Exploration of Cation Substitution in the Layered Compound $CrWN_2$. *MRS Online Proc. Libr.* **2002**, *755*, 631.
(27) Jain, A.; Ong, S. P.; Hautier, G.; Chen, W.; Richards, W. D.; Dacek, S.; Cholia, S.; Gunter, D.; Skinner, D.; Ceder, G.; Persson, K. A. Commentary: The Materials Project: A Materials Genome Approach to Accelerating Materials Innovation. *APL Mater.* **2013**, *1*, 011002.
(28) Hargreaves, J. S. J. Heterogeneous Catalysis with Metal Nitrides. *Coord. Chem. Rev.* **2013**, *257*, 2015−2031.
(29) Mazumder, B.; Chirico, P.; Hector, A. L. Direct Solvothermal Synthesis of Early Transition Metal Nitrides. *Inorg. Chem.* **2008**, *47*, 9684−9690.
(30) Odahara, J.; Sun, W.; Miura, A.; Rosero-Navarro, N. C.; Nagao, M.; Tanaka, I.; Ceder, G.; Tadanaga, K. Self-Combustion Synthesis of Novel Metastable Ternary Molybdenum Nitrides. *ACS Mater. Lett.* **2019**, *1*, 64−70.
(31) Mckay, D.; Hargreaves, J. S. J.; Rico, J. L.; Rivera, J. L.; Sun, X.-L. The Influence of Phase and Morphology of Molybdenum Nitrides on Ammonia Synthesis Activity and Reduction Characteristics. *J. Solid State Chem.* **2008**, *181*, 325−333.
(32) Hunter, S. M.; Mckay, D.; Smith, R. I.; Hargreaves, J. S. J.; Gregory, D. H. Topotactic Nitrogen Transfer: Structural Transformation in Cobalt Molybdenum Nitrides. *Chem. Mater.* **2010**, *22*, 2898−2907.
(33) Mckay, D.; Gregory, D. H.; Hargreaves, J. S. J.; Hunter, S. M.; Sun, X. Towards Nitrogen Transfer Catalysis: Reactive Lattice Nitrogen in Cobalt Molybdenum Nitride. *Chem. Commun.* **2007**, 3051.
(34) Arca, E.; Lany, S.; Perkins, J. D.; Bartel, C.; Mangum, J.; Sun, W.; Holder, A.; Ceder, G.; Gorman, B.; Teeter, G.; Tumas, W.; Zakutayev, A. Redox-Mediated Stabilization in Zinc Molybdenum Nitrides. *J. Am. Chem. Soc.* **2018**, *140*, 4293−4301.
(35) Kojima, R.; Aika, K. Molybdenum Nitride and Carbide Catalysts for Ammonia Synthesis. *Appl. Catal., A* **2001**, *219*, 141−147.
(36) Giordano, C.; Erpen, C.; Yao, W.; Antonietti, M. Synthesis of Mo and W Carbide and Nitride Nanoparticles via a Simple "Urea Glass" Route. *Nano Lett.* **2008**, *8*, 4659−4663.
(37) Giordano, C.; Erpen, C.; Yao, W.; Milke, B.; Antonietti, M. Metal Nitride and Metal Carbide Nanoparticles by a Soft Urea Pathway. *Chem. Mater.* **2009**, *21*, 5136−5144.
(38) Conway, J. O.; Prior, T. J. Interstitial Nitrides Revisited − A Simple Synthesis of M Mo_3N (M = Fe, Co, Ni). *J. Alloys Compd.* **2019**, *774*, 69−74.
(39) Hargreaves, J. S. J.; Mckay, D. A Comparison of the Reactivity of Lattice Nitrogen in Co_3Mo_3N and Ni2Mo3N Catalysts. *J. Mol. Catal. A: Chem.* **2009**, *305*, 125−129.
(40) *MDI Jade 9.5*; Materials Data. Inc.: Livermore, CA, USA, 2010.
(41) Jackson, S. K.; Layland, R. C.; zur Loye, H.-C. The Simultaneous Powder X-Ray and Neutron Diffraction Refinement of Two η-Carbide Type Nitrides, Fe_3Mo_3N and Co_3Mo_3N, Prepared by Ammonolysis and by Plasma Nitridation of Oxide Precursors. *J. Alloys Compd.* **1999**, *291*, 94−101.
(42) Alconchel, S.; Sapiña, F.; Beltrán, D.; Beltrán, A. Chemistry of Interstitial Molybdenum Ternary Nitrides $MnMo_3N$ (M=Fe, Co, N=3; M=Ni, N=2). *J. Mater. Chem.* **1998**, *8*, 1901−1909.
(43) Vegard, L. Die Konstitution Der Mischkristalle Und Die Raumfüllung Der Atome. *Z. Phys.* **1921**, *5*, 17−26.
(44) Magomedov, M. N. On the Deviation from the Vegard's Law for the Solid Solutions. *Solid State Commun.* **2020**, *322*, 114060.
(45) Perret, N.; Alexander, A.-M.; Hunter, S. M.; Chung, P.; Hargreaves, J. S. J.; Howe, R. F.; Keane, M. A. Synthesis,

https://doi.org/10.1021/acs.chemmater.3c00606
Chem. Mater. XXXX, XXX, XXX−XXX

Characterisation and Hydrogenation Performance of Ternary Nitride Catalysts. *Appl. Catal., A* **2014**, *488*, 128−137.
(46) Wang, C.; Qi, W.; Zhou, Y.; Kuang, W.; Azhagan, T.; Thomas, T.; Jiang, C.; Liu, S.; Yang, M. Ni-Mo Ternary Nitrides Based One-Dimensional Hierarchical Structures for Efficient Hydrogen Evolution. *Chem. Eng. J.* **2020**, *381*, 122611.
(47) Schmitt, C.; Giebeler, L.; Schierholz, R.; Endres, S.; Fasel, C.; Vogel, H.; Fuess, H. Characterization of V-W and Mo-W Mixed Oxide Catalysts for the Selective Oxidation of Acrolein to Acrylic Acid. *Z. Phys. Chem.* **2007**, *221*, 1525−1548.
(48) Jie, S.; Lin, X.; Chao, Z.; Liu, Z. Effective Ternary Copper-Cerium-Cobalt Catalysts Synthesized via a Modified Pechini Method for Selective Oxidation of Ethylbenzene. *Mater. Chem. Phys.* **2018**, *214*, 239−246.
(49) Weil, K. S.; Kumta, P. N. Synthesis of Ternary Transition Metal Nitrides Using Chemically Complexed Precursors. *Mater. Sci. Eng. B* **1996**, *38*, 109−117.
(50) Zhang, C.; Guo, H.; Gao, Y.; Gong, Y.; Jin, C.; He, J. Controllable Synthesis of Co_3W_3N Supporting on N-Doped GO as Electrocatalysts for Oxygen Reduction Reaction. *Chem. Phys. Lett.* **2022**, *793*, 139429.
(51) Weil, K. S.; Kumta, P. N. Synthesis and Structural Investigation of a New Ternary Transition Metal Nitride, Co_3W_3N. *J. Alloys Compd.* **1998**, *265*, 96−103.
(52) Subramanya Herle, P.; Vasanthacharya, N. Y.; Hegde, M. S.; Gopalakrishnan, J. Synthesis of new transition metal nitrides, MWN2 (M Mn, Co, Ni). *J. Alloys Compd.* **1995**, *217*, 22−24.
(53) Panda, R. N.; Dalavi, S. B.; Theerthagiri, J. Synthesis of High Surface Area W_2N and Co−W−N Nitrides by Chemical Routes. *Adsorpt. Sci. Technol.* **2012**, *30*, 345−354.
(54) Thomas, G. S.; Kamath, P. V. Line Broadening in the PXRD Patterns of Layered Hydroxides: The Relative Effects of Crystallite Size and Structural Disorder. *J. Chem. Sci.* **2006**, *118*, 127−133.
(55) Bréger, J.; Jiang, M.; Dupré, N.; Meng, Y. S.; Shao-Horn, Y.; Ceder, G.; Grey, C. P. High-Resolution X-Ray Diffraction, DIFFaX, NMR and First Principles Study of Disorder in the Li_2MnO_3−$Li[Ni_{1/2}Mn_{1/2}]O_2$ Solid Solution. *J. Solid State Chem.* **2005**, *178*, 2575−2585.
(56) Shaw, J.; Staddon, B. W. A Conductimetric Method for the Estimation of Small Quantities of Ammonia. *J. Exp. Biol.* **1958**, *35*, 85−95.

https://doi.org/10.1021/acs.chemmater.3c00606
Chem. Mater. XXXX, XXX, XXX−XXX